

VISTA Variables in the Via Lactea (VVV): The public ESO near-IR variability survey of the Milky Way

D. Minniti^{1,2,†}, P. W. Lucas^{3,†}, J. P. Emerson^{4,†}, R. K. Saito¹, M. Hempel¹,
P. Pietrukowicz^{1,5}, A. V. Ahumada^{6,7,8}, M. V. Alonso⁶, J. Alonso-García⁹,
J. I. Arias¹⁰, R. M. Bandyopadhyay¹¹, R. H. Barbá¹⁰, B. Barbuy¹², L. R. Bedin¹³,
E. Bica¹⁴, J. Borissova¹⁵, L. Bronfman¹⁶, G. Carraro⁷, M. Catelan¹, J. J. Clariá⁶,
N. Cross¹⁷, R. de Grijs^{18,19}, I. Dékány²⁰, J. E. Drew^{3,21}, C. Fariña²²,
C. Feinstein²², E. Fernández Lajús²², R. C. Gamen¹⁰, D. Geisler²³, W. Gieren²³,
B. Goldman²⁴, O. A. Gonzalez²⁵, G. Gunthardt¹⁰, S. Gurovich⁶, N. C. Hambly¹⁷,
M. J. Irwin²⁶, V. D. Ivanov⁷, A. Jordán¹, E. Kerins²⁷, K. Kinemuchi^{10,23},
R. Kurtev¹⁵, M. López-Corredoira²⁸, T. Maccarone²⁹, N. Masetti³⁰, D. Merlo⁶,
M. Messineo^{31,32}, I. F. Mirabel^{33,34}, L. Monaco⁷, L. Morelli³⁵, N. Padilla¹,
T. Palma⁶, M. C. Parisi⁶, G. Pignata³⁶, M. Rejkuba²⁵, A. Roman-Lopes¹⁰,
S. E. Sale²¹, M. R. Schreiber¹⁵, A. C. Schröder^{37,38}, M. Smith³⁹, L. Sodr e Jr.¹²,
M. Soto¹⁰, M. Tamura⁴⁰, C. Tappert¹, M. A. Thompson³, I. Toledo¹ &
M. Zoccali¹

(Affiliations can be found after the references)

†*Email addresses:* dante@astro.puc.cl (D. Minniti),
P.W.Lucas@herts.ac.uk (P. W. Lucas), j.p.emerson@qmul.ac.uk (J. P. Emerson)

Abstract

We describe the public ESO near-IR variability survey (VVV) scanning the Milky Way bulge and an adjacent section of the mid-plane where star formation activity is high. The survey will take 1929 hours of observations with the 4-metre VISTA telescope during five years (2010 – 2014), covering $\sim 10^9$ point sources across an area of 520 deg^2 , including 33 known globular clusters and ~ 350 open clusters. The final product will be a deep near-IR atlas in five passbands ($0.9 - 2.5 \mu\text{m}$) and a catalogue of more than 10^6 variable point sources. Unlike single-epoch surveys that, in most cases, only produce 2-D maps, the VVV variable star survey will enable the construction of a 3-D map of the surveyed region using well-understood distance indicators such

as RR Lyrae stars, and Cepheids. It will yield important information on the ages of the populations. The observations will be combined with data from MACHO, OGLE, EROS, VST, Spitzer, HST, Chandra, INTEGRAL, WISE, Fermi LAT, XMM-Newton, GAIA and ALMA for a complete understanding of the variable sources in the inner Milky Way. This public survey will provide data available to the whole community and therefore will enable further studies of the history of the Milky Way, its globular cluster evolution, and the population census of the Galactic Bulge and center, as well as the investigations of the star forming regions in the disk. The combined variable star catalogues will have important implications for theoretical investigations of pulsation properties of stars.

Key words: Surveys, Stars: variables: general, Galaxy: bulge, Galaxy: disk
PACS: 95.80.+p, 97.30.-b, 98.35.Jk, 98.35.Ln

1 Introduction

The bulk of the stars, gas and dust in the Milky Way are confined to its bulge and plane. As a result, in these directions, the extinction and crowding are high, making any study of the inner structure of the Galaxy difficult. Knowing how the stellar populations are distributed within the Galaxy is essential for such studies and hence the main goal of the described survey. Traditional distance indicators have been used with various success in the past. The approach was to concentrate on clear “windows”, where optical surveys can be carried out (e.g., MACHO, OGLE, EROS). In this paper we describe the VISTA Variables in the Via Lactea (VVV) survey¹, an ESO (European Southern Observatory) public near-IR variability survey. Its area includes the Milky Way bulge and an adjacent section of the mid-plane where star-formation activity is high. This survey will be conducted in the period 2010 – 2014 and will map the whole bulge systematically for multiple epochs.

We plan to cover a 520 deg^2 area (Fig. 1) containing $\sim 10^9$ point sources. Our survey will give the most complete catalogue of variable objects in the bulge, with more than $\sim 10^6$ variables. Chief among them are the RR Lyrae, which are accurate primary distance indicators, and well understood regarding their chemical, pulsational and evolutionary properties. For the sake of space and coherence we concentrate on the RR Lyrae and the star clusters, noting that similar studies can be done for many of the other populations of variable objects.

Earlier single-epoch near-IR surveys (e.g., COBE, 2MASS, GLIMPSE) have proven that the Galactic bulge is triaxial and boxy, and contains a bar (Dwek et al. ,

¹Detailed information about the VVV survey can be found in <http://vvvsurvey.org/>

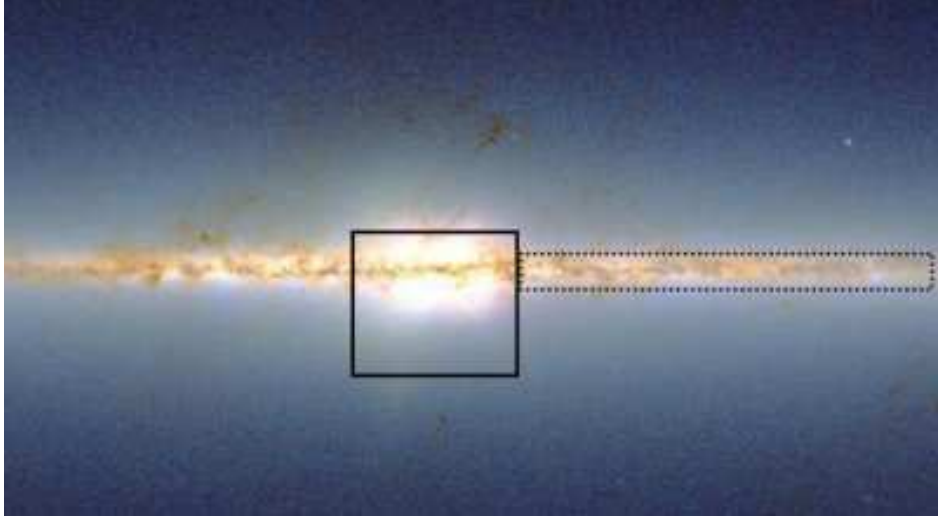


Figure 1: 2MASS map of the inner Milky Way showing the VVV bulge (solid box, $-10^\circ < l < +10^\circ$ and $-10^\circ < b < +5^\circ$) and plane survey areas (dotted box, $-65^\circ < l < -10^\circ$ and $-2^\circ < b < +2^\circ$).

1995; López-Corredoira et al., 2005; Benjamin et al., 2005). Presently, the only model we have for the formation of boxy/barred bulges is through secular evolution of a pre-existing disk. This scenario is believed to be the dominant channel of formation of bulges in late-type spirals (Sbc), whereas early-type spiral bulges (S0/Sa) show structural and kinematic evidence for an early, rapid collapse, which seems to be confirmed by the old age of their stellar populations (e.g., Kormendy & Kennicutt, 2004).

However, the best-studied spiral bulge, that of the Milky Way, is precisely the most problematic one to understand in this context. While its surface brightness shows a barred structure, its stellar population is predominantly old (Kuijken & Rich, 2002; Zoccali et al., 2003) and has α -element enhancement, characteristic of rapid formation. Nevertheless, the high mean age of the Bulge still leaves space for a small fraction of young stellar objects (YSO) which have been found in the inner Bulge (e.g., Schuller et al., 2006; Yusef-Zadeh et al., 2009). This is in agreement with the results of Zoccali et al. (2006) which indicate that the chemical composition of the bulge stars is different from that of both thin and thick-disk stars. Thus, the predictions from the formation of the Milky Way bulge through secular evolution of the disk seem to be in conflict with some key properties of its stellar population. However, Meléndez et al. (2008) recently published results that are in contradiction to Zoccali et al. (2006) and show that bulge and disk stars are indis-

tinguishable in their chemical composition. Given that the near-IR colours depend strongly on metallicity, the VVV survey will help us to investigate the metallicity distribution in the survey region. Spectroscopic data (e.g., future APOGEE; Majewski et al., 2007) will provide additional α -element abundances.

Our survey of the RR Lyrae in the Galactic bulge will allow us to map its 3-D structure (as shown by Carney et al., 1995) and will provide key information on the age of its population, given that RR Lyrae stars are tracers of the old population (e.g., Catelan, 2004b, 2009, and references therein). This will enable us to combine the ages of the stellar populations with their spatial distributions. We note that most single-epoch surveys only provide 2-D maps. With the present survey, the peak and width of the RR Lyrae distribution is expected to be measured with an accuracy of better than 0.01 mag, which is the required precision to determine the 3-D structure not only of the bulge, but also of the Sagittarius dwarf spheroidal galaxy (Sgr dSph) located behind the Milky Way (e.g., Alard, 1996) and included in our survey.

At the same time, a comparison between the RR Lyrae (and type II Cepheids) in the field and in globular clusters may hold precious information about the formation of the bulge (e.g. Feast et al., 2008). Modern Λ CDM cosmology predicts that large galaxies such as the Milky Way formed by accretion of hundreds of smaller “protogalactic fragments”, perhaps not unlike the progenitors of the present-day dwarf spheroidal satellites (e.g., Abadi et al., 2003). Interestingly, two very massive globular clusters in the Galactic bulge, NGC 6388 and NGC 6441, have recently been suggested to be the remnants of dwarf galaxies that were accreted in the course of the Galaxy’s history (Ree et al., 2002). These clusters might prove similar to the cases of M54 (NGC 6715), in the center of the Sgr dSph, which is currently being cannibalised by the Milky Way (Ibata et al., 1995), and of ω Cen (NGC 5139), which has long been suspected to be the remnant nucleus of a dwarf galaxy (e.g., Altmann et al., 2005, and references therein). Our proposed search for RR Lyrae and type II Cepheids in the Galactic bulge will reveal the presence of debris related to the accretion events that might have left behind NGC 6441 as remnant object. The latter is part of our survey.

In order to understand the Milky Way’s populations globally, it is necessary to survey the inner Galactic plane as well. Therefore, we will survey an adjacent region of the mid-plane and provide a Legacy Database and 3-D atlas of a large Population I (i.e. young and luminous stars) region. We have selected the region $-65^\circ < l < -10^\circ$ and $|b| < 2^\circ$ (see Fig. 1), where star-formation activity is high and for which there will be complementary optical, mid-IR, and far-IR data from VPHAS+, the Spitzer, GLIMPSE and MIPS GAL surveys, and from the all-sky AKARI and WISE survey. The addition of this region will also permit us to discriminate between various models of the inner Galactic structure which, besides the triaxial bulge, contain a long bar and a ring (e.g., López-Corredoira et al., 2007,

and references therein) or not (e.g., Merrifield, 2004, and references therein). Indeed, the selected region includes the putative negative-longitude tip of the long bar (at $l \approx -14^\circ$, $|b| < 1^\circ$), which has not yet been observed.

The large survey area will allow several remaining astrophysical problems to be addressed. For example, the effect of the environment on star formation and in particular the initial mass function (IMF) at low masses is presently poorly known. This issue will be addressed statistically by observing hundreds of star-forming regions and cross-correlating the shapes of their luminosity functions with cluster density, the presence of high-mass stars, and galactocentric distance. For comparison, VVV survey will reach 1 *mag* deeper than UKIDSS Galactic Plane Survey (GPS), which overlaps with VVV in the region of $-2^\circ < l < +10^\circ$, $|b| < 2^\circ$. Other important parameters, such as velocity dispersion and metallicity, will be determined by spectroscopic follow-up observations. In addition, the luminosity function of the clusters themselves will be measured, for both star-forming clusters and more evolved open clusters.

These issues cannot be addressed with optical surveys, owing to the high extinction in the plane. The Spitzer data will be invaluable for detecting the most obscured high-mass protostars within star-forming regions. A near-IR survey will be more sensitive to all but the reddest objects, and the superior spatial resolution in these wavebands will be essential for resolving distant clusters and the crowded field populations.

2 Technical description

2.1 Telescope and instrument design

The Visible and Infrared Survey Telescope for Astronomy (VISTA) is a 4m-class “wide-field” telescope located at ESO’s Cerro Paranal Observatory in Chile, designed to conduct large-scale surveys of the southern sky at near-IR wavelengths (0.9 to 2.5 μm). The telescope has an altitude-azimuth mount, and quasi Ritchey-Chrétien optics. An $f/1$ primary mirror was designed together with Cassegrain-focus instrumentation to offer the best solution to the difficult problem of combining a wide-field with good image quality, and results in a physically large focal plane with an $f/3.25$ focus (McPherson et al., 2006). VISTA’s active optics uses two low-order curvature sensors, which operate concurrently with science exposures, and a high-order curvature sensor.

The telescope is equipped with a near-IR camera containing 67 million pixels (an array of $16 \times 2048 \times 2048$ Raytheon VIRGO IR detectors) of mean size $0''.34$ and available broad-band filters at $ZYJHK_s$ and a narrow-band filter at 1.18 μm . Given VISTA’s nominal pixel size, the diameter of the field of view is 1.65 deg. The

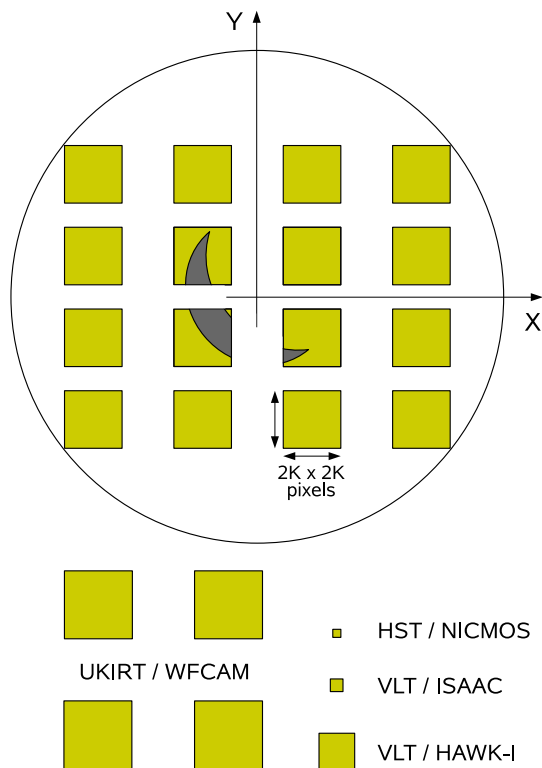


Figure 2: Diagram showing the array of the sixteen detectors on the VISTA camera and the axis orientation used to shift the camera in each exposure to obtain the tiles. For comparison we show the crescent Moon over the VISTA camera and the fields of view of UKIRT/WFCAM, HST/NICMOS, VLT/ISAAC, and VLT/HAWK-I.

point-spread function (PSF) of the telescope+camera system (including pixels) is designed to have a full width at half maximum (FWHM) of $0''.51$, not including the contribution of atmospheric turbulence. Seeing, and other weather-related statistics for Cerro Paranal, are given at ESO's "Astroclimatology of Paranal" web pages². The VISTA site is expected to have similar conditions, which are well suited to our survey requirements.

The 16 detectors in the camera are not buttable and are arranged as shown in Figure 2. Each individual exposure produces a sparsely sampled image of the sky known as a "pawprint", covering an area of 0.599 deg^2 .

To 'fill in' the gaps between the detectors to produce a single filled "tile" with reasonably uniform sky coverage, the minimum number of pointed observations

²<http://www.eso.org/gen-fac/pubs/astclim/paranal/>

(with fixed offsets) required is six (three offsets in Y and two offsets in X). After six steps an area of 1.501 deg^2 on the sky, corresponding to one tile, is (almost) uniformly covered.

2.2 Data reduction

We will use the enhanced VISTA Data Flow System³ (VDFS; Emerson et al., 2004; Irwin et al., 2004; Hambly et al., 2004). It includes all basic data reduction steps:

- (i) removing instrumental signature (bias and dark frames, twilight, and dome flatfields, linearity, bad pixel maps, cross-talk, gain calibrations), merging paw-prints into tiles and calibrating photometrically and astrometrically;
- (ii) extracting source catalogues on a tile-by-tile basis;
- (iii) constructing survey-level products – stacked pixel mosaics, difference images, and merged catalogues;
- (iv) providing the team with both data access and methods for querying and analyzing the data; and
- (v) producing virtual observatory (VO)-compliant data products for delivery to the ESO archive.

Figure 3 shows a flow chart of the data processing. The pipeline products are: astrometrically corrected and photometrically calibrated tiles in each filter used, confidence maps, and homogeneous object catalogues (Cross et al., 2009). The pipeline records the processing history and calibration information of each file, including calibration files and quality control parameters. The Cambridge Astronomy Survey Unit (CASU) component of the VDFS will be responsible for the basic pipeline processing and the first calibration, all done on a daily basis.

2.3 Combination/image subtraction (archive)

The “second”-order data processing requires access to larger sets of data to produce survey products. It is carried out by the Wide Field Astronomy Unit’s (WFAU) VISTA Science Archive (VSA) in Edinburgh. The Science Archive contains only calibrated data and catalogues, and no raw data. The Science Archive is responsible for:

- (i) image stacking to produce combined and differenced tiles and source merging;
- (ii) quality control: assessment of the data quality and filtering of the data that do not meet the established criteria for photometric and astrometric accuracy;

³The VISTA Data Flow System (VDFS) is a collaboration between the UK Wide Field Astronomy Unit at Edinburgh (WFAU) and Cambridge Astronomy Survey Unit (CASU), coordinated by the VISTA PI and funded for VISTA by the Science and Technology Facilities Council.

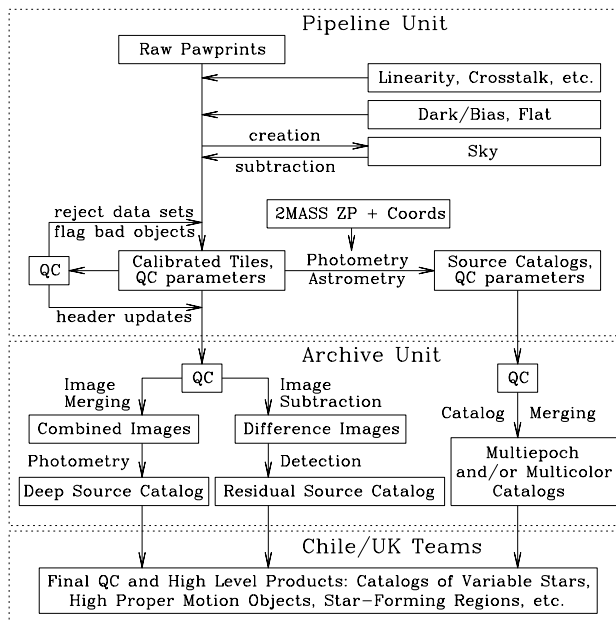


Figure 3: Flow chart of the VVV data processing (QC: Quality Control; ZP: Zero-point).

(iii) light-curve extraction: this will be done by implementing an image-subtraction algorithm (Alard & Lupton, 1998; Alard, 2000), which will allow us to create the catalogue of variable sources. This method provides excellent results for crowded fields in which the traditional aperture or PSF-fitting photometry fails (e.g., Kaluzny et al., 2004; Pietrukowicz et al., 2005).

2.4 Photometric calibration

During the first period we will carry out the external calibrations and transformations to the standard system using 2MASS and UKIDSS for bootstrapping⁴.

The calibration scheme for a given filter is as follow:

$$m_{\text{cal}} = m_{\text{inst}} + ZP - k(X - 1) = m_{\text{std}} + cl_{\text{std}} \quad (1)$$

where m_{cal} is the calibrated magnitude, m_{inst} the measured instrumental magnitude, ZP the zeropoint, k the extinction coefficient, and X the airmass of the object. On

⁴The filter transmission curves for each instrument can be found at <http://www.vista.ac.uk/index.html> (VISTA), http://web.ipac.caltech.edu/staff/waw/2mass/opt_cal/index.html (2MASS) and <http://www.ukidss.org/technical/instrument/filters.html> (UKIDSS).

the right-hand side of this equation, m_{std} and clr_{std} are the corresponding standard magnitude and colour.

Calibration and quality control is done using 2MASS stars in the frames themselves, applying colour equations to convert 2MASS photometry to the VISTA photometric system (Skrutskie et al., 2006; Hodgkin et al., 2009).

There are thousands of unsaturated 2MASS stars in $JH K_s$ with photometric errors <0.1 mag in every VISTA tile field. A large fraction of these can be sufficiently isolated even in the crowded fields.

To calibrate the Y - and Z -band data (both filters are not available from 2MASS) we will use observations of the standard VISTA calibration fields as required by the ESO Public Survey Panel. Details will be published in a forthcoming paper describing the science verification.

The internal gain correction applied through flat-fielding will place the detectors on a common zero-point system. After deriving this ZP in each tile, a double check using the overlap regions will be made to estimate the internal photometric accuracy.

3 Observing strategy

The VISTA tile field of view is 1.501 deg^2 , hence 196 tiles are needed to map the bulge area and 152 tiles for the disk⁵. Adding some X and Y overlap between tiles for a smooth match, the area of our unit tile covered twice is 1.458 deg^2 . Figure 4 provides a schematic representation of the tiling scheme for the Galactic center region.

The variability study in the bulge will be carried out in the K_s band down to ~ 18 mag (signal-to-noise ≈ 3). The total exposure time for a VISTA tile field is 162 s. Our strategy yields about 30 deg^2 per hour, or 300 deg^2 per night. The combined epochs will reach $K_s = 20$ mag, which is three magnitudes fainter than the unreddened bulge main-sequence turn-off (MS turn-off), although the densest fields will be confusion-limited. However, applying both PSF fitting and image subtraction, we will recover the light curves of most objects down to $K_s = 18$ mag, even in moderately crowded fields. This is more than 3 mag fainter than the unreddened known RR Lyrae in the Galactic bulge. We expect to find RR Lyrae even in fields with $A_V = 10$ mag.

Table 1 lists some reference K_s -band magnitudes at the distance of the bulge for a range of extinction and reddening values. These typical magnitudes were obtained from Carney et al. (1995), Alard (1996), Alcock et al. (1998), and Zoccali et al.

⁵The tiles' spacing and orientation were calculated with the Survey Area Definition Tool (SADT) software to maximize the efficiency of the sky coverage. See <http://www.vista.ac.uk/observing/sadt/>

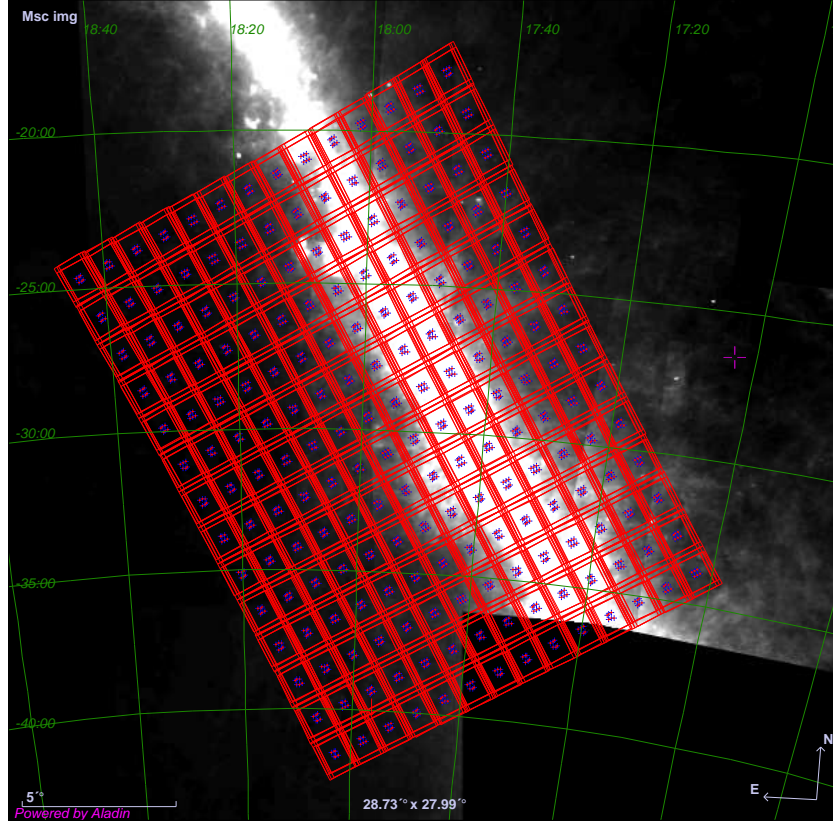


Figure 4: Coverage of the Galactic center region overlaid on a mid-IR map. Boxes mark the tiles needed to cover the bulge area (see Fig. 1), whereas the crosses mark the box centers.

(2003). As a reference point, for Baade’s window $E(B - V) = 0.5$ mag, so that $A_V = 1.5$, $A_J = 0.4$, and $A_K = 0.2$ mag (Rieke & Lebofsky, 1985). This table shows that the tip of the bulge red-giant branch (RGB) will saturate ($K_s < 9.5$), but for the RGB clump giants, and even for the tip of the RGB of the Sgr dSph galaxy, the VVV survey will be able to see giants throughout the bulge, even in the most obscured regions. The bulge RR Lyrae and the Sgr dSph galaxy red-clump giants will also be detected, even for the regions with the highest extinction ($A_V > 30$ mag) at low Galactic latitudes. Finally, the RR Lyrae of the Sgr dSph galaxy and the bulge MS turn-off stars will be detected only in the regions with low absorption ($A_V < 10$ mag) at higher latitudes. We are aware that the use of an ‘universal’ extinction law $A_V = 3.1 E(B - V)$ is problematic in the inner region of the bulge. According to Nishiyama et al. (2006) and Gosling et al. (2009) a single

extinction law is not consistent with the observations of the Galactic center along different lines of sight.

For the plane survey, the K_s -band observations require a total time of 80 s on target, and an elapsed time of 366 s per tile.

Bright point sources with $K_s < 9.5$ mag will be saturated in the individual images. This will therefore include most unreddened bulge Mira variables, but Miras in the Sgr dSph galaxy can be monitored, as well as Miras located in regions with very high extinction (e.g., next to the Galactic center). The Mira population in the Galactic center has been studied by Matsunaga et al. (2009). In addition, bright-star saturation may be an issue, but we estimate that even in the worst cases only a small portion of the field will be rendered useless. Hence we do not expect that the saturation of the brightest stars to effect our conclusions about three-dimensional structure of the inner Milky Way. For example, in the optical microlensing surveys where CCD bleeding is comparatively worse, less than 5% of the most crowded bulge fields are lost.

To illustrate the precision of crowded-field IR photometry we include Fig. 5, showing photometry of the planetary transit OGLE-TR-113 obtained with NTT/SOFI (top panel), and photometric accuracy of those observations as a function of magnitude (bottom panel). In order to evaluate the amplitude threshold for our detections, we have carried out Monte Carlo simulations using the RR Lyrae light curve templates from Jones et al. (1996) and Del Principe et al. (2005). As a result, we find that, at a typical magnitude of $K_s \approx 15 - 16$, and taking into account the expected photometric errors, we should be able to detect RR Lyrae stars with amplitudes down to $A_K = 0.05 - 0.07$ mag using 80 datapoints from the first three years of VVV operation, and further down to $A_K = 0.03 - 0.05$ mag if the dataset is extended to cover 180 phase points over a time frame of 5 years.

The total estimated time per observing period is given in Table 2, which also shows the requirements for Moon, seeing, and transparency conditions. The times include overheads (both for readout and for changing to a new tile) and time possibly spent on standard stars for the Z and Y observations (not used in the 2MASS and UKIDSS survey). This strategy allows us to provide various data to the community, enabling follow-up throughout the survey. The full survey will require a total of 192 nights of observations over 5 years. A schematic schedule of the survey is shown in Fig. 6.

During the first year, the whole bulge area will be observed in the K_s band for 6 consecutive epochs, for a total of 65 hours. A further 86 hours will be devoted to complete imaging of each bulge tile in $ZYJH$. This will provide reliable near-simultaneous fluxes and colours for each tile area.

The same strategy will be applied to the 152 tiles covering the disk area for the single-epoch and the quasi-simultaneous multi-colour disk survey. The total

Table 1: K_s -band magnitudes at the distance of the bulge. The absorption values are based on the standard extinction law as derived by Rieke & Lebofsky (1985).

| | $E(B - V)=0$ | $E(B - V)=0.5$ | $E(B - V)=1.5$ | $E(B - V)=3.2$ | $E(B - V)=4.8$ | $E(B - V)=8.4$ |
|--------------------|---------------|----------------|----------------|----------------|-------------------|-------------------|
| | $A_V = 0$ | $A_V = 1.5$ | $A_V = 5.0$ | $A_V = 10.0$ | $A_V = 15.0$ | $A_V = 26.3$ |
| | $A_J = 0$ | $A_J = 0.4$ | $A_J = 1.4$ | $A_J = 2.8$ | $A_J = 4.2$ | $A_J = 7.4$ |
| Population | $A_K = 0$ | $A_K = 0.2$ | $A_K = 0.6$ | $A_K = 1.1$ | $A_K = 1.7$ | $A_K = 3.0$ |
| Bulge RGB tip | $K_s = 8.0^*$ | $K_s = 8.2^*$ | $K_s = 8.6^*$ | $K_s = 9.1^*$ | $K_s = 9.7$ | $K_s = 11.0$ |
| Sgr dSph RGB tip | $K_s = 10.5$ | $K_s = 10.7$ | $K_s = 11.1$ | $K_s = 11.6$ | $K_s = 12.2$ | $K_s = 13.5$ |
| Bulge RGB clump | $K_s = 12.9$ | $K_s = 13.1$ | $K_s = 13.5$ | $K_s = 14.0$ | $K_s = 14.6$ | $K_s = 15.9$ |
| Bulge RR Lyrae | $K_s = 14.3$ | $K_s = 14.5$ | $K_s = 14.9$ | $K_s = 15.4$ | $K_s = 16.0$ | $K_s = 17.3$ |
| Sgr dSph RGB clump | $K_s = 15.4$ | $K_s = 15.6$ | $K_s = 16.0$ | $K_s = 16.5$ | $K_s = 17.1$ | $K_s = 18.4^{**}$ |
| Sgr dSph RR Lyrae | $K_s = 16.8$ | $K_s = 17.0$ | $K_s = 17.4$ | $K_s = 17.9$ | $K_s = 18.5^{**}$ | $K_s = 19.8^{**}$ |
| Bulge MS turn-off | $K_s = 17.0$ | $K_s = 17.2$ | $K_s = 17.6$ | $K_s = 18.1$ | $K_s = 18.7^{**}$ | $K_s = 20.0^{**}$ |

* saturated

** beyond detection

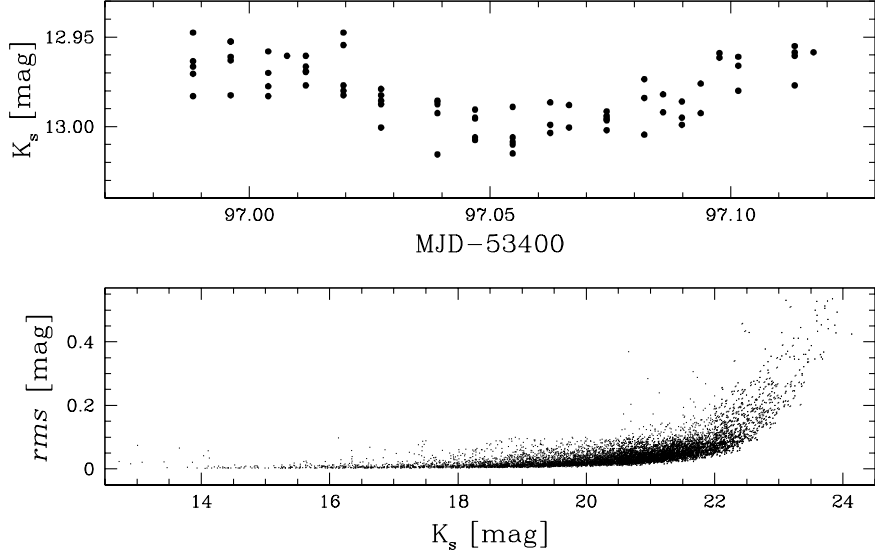


Figure 5: Top panel: Light curve of the planetary transit OGLE-TR-113 measured with SOFI at the 3.5-m ESO NTT telescope in the K_s band. This star is located in the Galactic plane in the field of Carina, a moderately crowded region. Bottom panel: Precision of the relative photometry obtained with SOFI as a function of magnitude. The magnitudes and rms are calculated in two iterations, removing the $> 10\sigma$ outliers.

time spent on the disk for the first year is thus 141 hours. Added to the 151 hours for the bulge, we will thus spend 292 hours in total on the survey during the first year. The multi-color observations, in combination with datasets from UKIDSS GPS (near IR), VST/VPHAS+ (optical) and GLIMPSE and GLIMPSE-II (mid-IR), will be used to build improved extinction maps for the survey region. Note that the individual, single-epoch observation blocks (OBs) in K_s all have the same limiting depth (under the same conditions), whether forming part of the VVV’s bulge or disk components.

Being fully aware of the confusion and background limits, the observing plan would cycle alternately through fields of varying density for optimal sky subtraction. The filter order in the OBs will be optimized to minimize overheads.

During the second year, we will acquire another 20 epochs in K_s for the whole bulge (217 hours) and 10 for the plane (75 hours), for a total of 292 hours. These additional epochs will improve our ability to detect variable sources (but will not permit us to conclusively establish the variability phases, at least for many of the RR Lyrae stars). These data will also allow the creation of deeper master maps in

Table 2: Estimated observing time for the full survey.

| Year | Time [h] | RA range [hh:mm] | Moon | Seeing ["] | Transparency | Number of K-band epochs |
|--------|----------|------------------|------|--------------|--------------|-------------------------|
| year 1 | 292 | 12:00–19:00 | any | 0.8 | clear | 6 (bulge and disk) |
| year 2 | 292 | 12:00–19:00 | any | 0.8 | clear | 4 (bulge and disk) |
| year 3 | 652 | 12:00–19:00 | any | any | thin | 80 (bulge only) |
| year 4 | 525 | 12:00–19:00 | any | any | thin | 70 (disk only) |
| year 5 | 168 | 12:00–19:00 | any | 0.8 | clear | 20 (bulge) + 9 (disk) |
| Total | 1929 | | | | | |

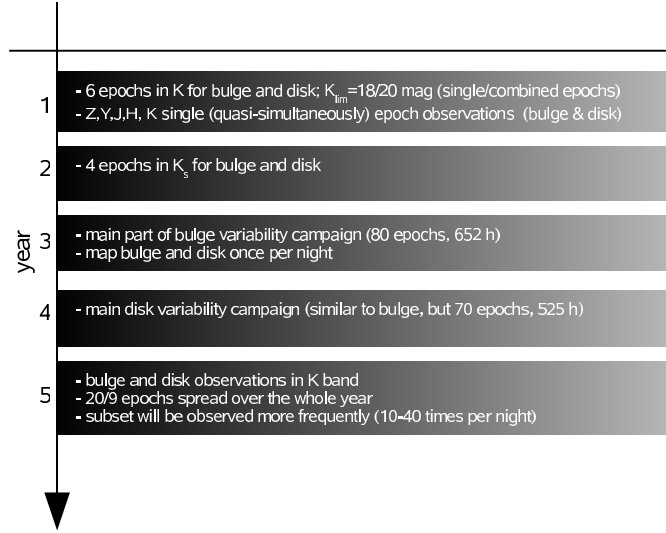


Figure 6: Schematic schedule of the VVV survey strategy.

K_s , to fine tune the strategy for the main campaign of the following year.

During the third year, the main bulge-variability campaign of 60 epochs will be carried out over 652 hours. According to the ESO Public Survey requirements, only 40 nights can be consecutive, while the others will be spread over the bulge season. We will use the K_s band to map the whole bulge and inner plane. A subset of the fields can be observed more frequently (4–8 times per night). This strategy allows us to partially remove aliasing and to improve the periods, while being more sensitive to shorter timescale variables and microlensing events.

During the fourth year, the main Galactic-plane variability campaign will be carried out over 70 epochs using 525 hours in K_s , following a similar strategy as for the bulge in the previous year. According to the ESO requirements, only part of these observations can be carried out over 27 consecutive nights.

Finally, during the fifth year, we will acquire 12 more epochs for the bulge and five more for the disk, with observations spread over the season, taking a total of 130 and 38 hours, respectively. This allows measurements of longer-timescale variables, and the search for high-proper-motion objects. A subset of the fields can be observed much more frequently (10–40 times per night). This strategy enables detection of short-period variables and planetary transits.

4 Scientific goals

The major VVV survey products will be a high-resolution $ZYJHK_s$ colour atlas of the bulge and plane regions, and a catalogue of variable point sources, including positions, mean magnitudes, and amplitudes. We expect to detect more than 10^6 variable objects. However, the total number may even reach 10^7 if one takes into account results from recent deep variable searches in optical bands in selected Galactic-plane regions (Weldrake & Bayliss, 2008; Pietrukowicz et al., 2009). Our database will be public, a significant treasure for the whole community to exploit for a variety of scientific programmes.

The main scientific goals of the VVV survey are:

1. *To find RR Lyrae in the bulge*, which will allow us to determine periods and amplitudes, and measure accurate mean K_s magnitudes. We will construct the Bailey diagram (luminosity amplitude vs. period), and interpret the results of the variability analysis in terms of stellar pulsation and evolution models, similarly to what is currently done using (primarily) the visual bandpasses (e.g., Bono et al., 2000, 2007; Marconi et al., 2003; Cacciari et al., 2005; Marconi & Degl’Innocenti, 2007). As pointed out by Bono et al. (2000), one common limitation in the comparison between hydrodynamical pulsation models and the observations is the lack of proper sampling in the available near-IR light curves – a situation which will be dramatically improved with the advent of the well-sampled K_s -band light curves from the VVV survey. Naturally, while RR Lyrae stars are the main focus of this project, similar such studies will be possible for many other types of variable stars, provided they are detected in significant numbers in our studied fields – including, for instance, classical Cepheids (Fiorentino et al., 2007), type II Cepheids (Di Criscienzo et al., 2007), anomalous Cepheids (Fiorentino et al., 2006), and Mi-

ras and semiregular variables (Kerschbaum et al., 2006; Smith et al., 2006), among others – with a significant impact also upon their use as distance indicators.

The pulsation properties of bulge variables will be compared with those of similar variables in the halo and nearby dwarf galaxies (e.g., Catelan, 2009). The distances measured and RR Lyrae counts can be compared with the red-clump giants, which are excellent tracers of the inner bar (Stanek et al., 1994). This would define the geometry of the inner bar and of additional structures (such as a potential second bar; Nishiyama et al., 2005), and explore the radial dependence of the density (e.g., Minniti et al., 1999), or trends with Galactic latitude-longitude, to finally unveil the structure of the bulge. The microlensing surveys that we have been involved in (OGLE and MACHO) have discovered a small fraction of the bulge RR Lyrae stars (e.g., Fig. 7, see Alcock et al., 1998; Woźniak et al., 2002). Our survey will increase the amount of data on bulge RR Lyrae significantly.

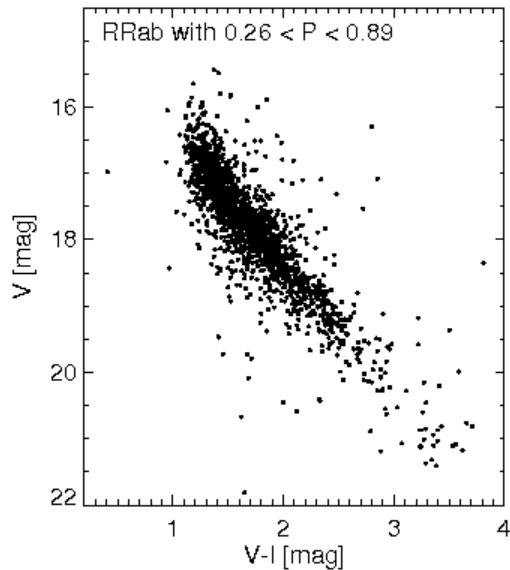


Figure 7: Optical colour-magnitude diagram for fundamental mode RR Lyrae stars in the Galactic bulge from the Optical Gravitational Lensing Experiment (Collinge et al., 2006)

We will search for RR Lyrae and type II Cepheids in the Galactic bulge to reveal the presence of any debris related to accretion events that might have left behind the present-day globular cluster NGC 6441. This globular cluster is well known to contain an anomalous RR Lyrae population, with periods that are much longer than those of known field RR Lyrae stars of similarly high metallicity (e.g.,

Pritzl et al., 2000, 2003). In particular, the presence of the unusually long-period ($P > 0.45$ d) RRc (first overtone) variables, which have so far not been found in the general field but are present in large numbers in this globular cluster (e.g., Catelan, 2004a), should provide the smoking gun for the presence of NGC 6441-related debris in the general bulge field. In a similar vein, long-period RRab stars (fundamental-mode pulsators) occupying the appropriate position in the period-amplitude diagram should also provide us with a strong indication of prior membership of such a protogalactic fragment.

2. *To identify variable stars belonging to known star clusters.* There are 33 globular clusters and 355 open clusters located in the VVV area (Fig. 8), which may contain RR Lyrae, type I and II Cepheids, semiregular variables, and eclipsing binaries, among other types of variables. Distances, reddening values, metallicities, and horizontal-branch (HB) types will be obtained for these clusters from a homogeneous dataset (e.g., Catelan et al., 2006; Zoccali et al., 2003). In some favourable cases, ages can be derived. Table 3 lists the globular clusters that will be covered, giving positions in equatorial and Galactic coordinates, and distances from the Sun. The asterisks in the last column indicate that more than one third of these clusters have uncertain distances. We will improve the distances for these globulars, and confirm the previous estimates for the rest of the open and globular cluster sample.

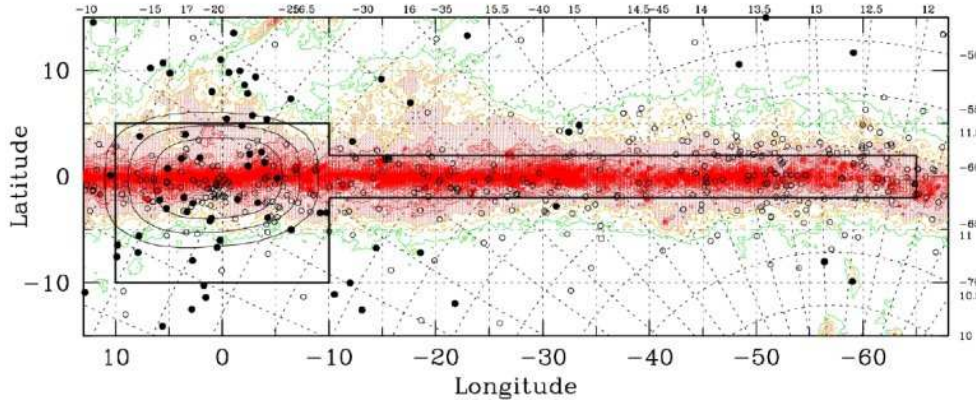


Figure 8: Map of the globular and open cluster positions (full and empty circles, respectively) towards the Milky Way bulge and plane. Included in the VVV area are the 33 globular clusters listed in Table 3 (Harris, 1996), and 355 open clusters (Bica et al., 2003; Dutra et al., 2003; Dias et al., 2006). The bulge contours are indicated.

Table 3: The 33 known globular clusters within the VVV area.

| Cluster ID | RA (J2000) [hh:mm:ss] | DEC (J2000) [dd:mm:ss] | l [deg] | b [deg] | D [kpc] |
|--------------|--------------------------|---------------------------|--------------|--------------|------------|
| Terzan 2 | 17:27:33.1 | -30:48:08 | 356.32 | 2.30 | 8.7 |
| Terzan 4 | 17:30:39.0 | -31:35:44 | 356.02 | 1.31 | 9.1 * |
| HP 1 | 17:31:05.2 | -29:58:54 | 357.42 | 2.12 | 14.1 * |
| Liller 1 | 17:33:24.5 | -33:23:20 | 354.84 | -0.16 | 9.6 * |
| NGC 6380 | 17:34:28.0 | -39:04:09 | 350.18 | -3.42 | 10.7 |
| Terzan 1 | 17:35:47.2 | -30:28:54 | 357.56 | 0.99 | 5.6 |
| Ton 2 | 17:36:10.5 | -38:33:12 | 350.80 | -3.42 | 8.1 * |
| NGC 6401 | 17:38:36.6 | -23:54:34 | 3.45 | 3.98 | 10.5 |
| Pal 6 | 17:43:42.2 | -26:13:21 | 2.09 | 1.78 | 5.9 |
| Djorg 1 | 17:47:28.3 | -33:03:56 | 356.67 | -2.48 | 12.0 * |
| Terzan 5 | 17:48:04.9 | -24:46:45 | 3.84 | 1.69 | 10.3 * |
| NGC 6440 | 17:48:52.7 | -20:21:37 | 7.73 | 3.80 | 8.4 |
| NGC 6441 | 17:50:12.9 | -37:03:05 | 353.53 | -5.01 | 11.7 |
| Terzan 6 | 17:50:46.4 | -31:16:31 | 358.57 | -2.16 | 9.5 * |
| NGC 6453 | 17:50:51.7 | -34:35:57 | 355.72 | -3.87 | 9.6 |
| UKS 1 | 17:54:27.2 | -24:08:43 | 5.12 | 0.76 | 8.3 * |
| Terzan 9 | 18:01:38.8 | -26:50:23 | 3.60 | -1.99 | 6.5 * |
| Djorg 2 | 18:01:49.1 | -27:49:33 | 2.76 | -2.51 | 6.7 * |
| Terzan 10 | 18:02:57.4 | -26:04:00 | 4.42 | -1.86 | 5.7 * |
| NGC 6522 | 18:03:34.1 | -30:02:02 | 1.02 | -3.93 | 7.8 |
| NGC 6528 | 18:04:49.6 | -30:03:21 | 1.14 | -4.17 | 7.9 |
| NGC 6540 | 18:06:08.6 | -27:45:55 | 3.29 | -3.31 | 3.7 |
| NGC 6544 | 18:07:20.6 | -24:59:51 | 5.84 | -2.20 | 2.7 |
| NGC 6553 | 18:09:17.6 | -25:54:31 | 5.25 | -3.03 | 6.0 |
| HJK2000-GC02 | 18:09:36.5 | -20:46:44 | 9.78 | -0.62 | 4.0 * |
| NGC 6558 | 18:10:17.6 | -31:45:50 | 0.20 | -6.02 | 7.4 |
| Terzan 12 | 18:12:15.8 | -22:44:31 | 8.36 | -2.10 | 4.8 * |
| NGC 6569 | 18:13:38.8 | -31:49:37 | 0.48 | -6.68 | 10.7 |
| NGC 6624 | 18:23:40.5 | -30:21:40 | 2.79 | -7.91 | 7.9 |
| NGC 6626 | 18:24:32.9 | -24:52:12 | 7.80 | -5.58 | 5.6 |
| NGC 6638 | 18:30:56.1 | -25:29:51 | 7.90 | -7.15 | 9.6 |
| NGC 6642 | 18:31:54.1 | -23:28:31 | 9.81 | -6.44 | 8.4 |
| NGC 6656 | 18:36:24.2 | -23:54:12 | 9.89 | -7.55 | 3.2 |

* uncertain distances

For some of the Cepheids which we expect to find in open clusters, we will derive improved distances by applying the IR surface-brightness technique (Gieren et al., 2005; Fouque & Gieren, 1997) on these variables.

3. *To find eclipsing binaries in large numbers.* We expect to detect more than 5×10^5 binaries, an unprecedented database that will allow us to determine periods, amplitudes, mean magnitudes, study stellar properties, and also select extrasolar planetary-transit candidates. In particular, YY Gem-like systems can be identified to constrain the lower main-sequence parameters (e.g., Torres & Ribas, 2002), and selected transit fields can be followed frequently to identify and measure extrasolar giant planets (Udalski et al., 2002).

4. *To find rare variable sources.* The massive variability dataset and multi-colour atlas will allow us to search for CVs (novae, dwarf novae) and other eruptive variables (e.g., RS CVn), eclipsing binary RR Lyrae, pre-HB/post He-flash stars (Silva Aguirre et al., 2008), eclipsing binary red-clump giants, luminous blue variables (LBVs), FU Ori protostars undergoing unstable accretion, and asymptotic giant branch (AGB) stars at the stage of unstable shell burning. The Murchison Widefield Array (Lonsdale et al., 2009) will soon open up the field of surveys of radio transients in the southern hemisphere, likely making infrared variability surveys of the southern part of the Galaxy interesting for interpreting their results. The Galactic center region contains numerous high energy sources without counterparts in the optical/infrared band, with continuing discoveries coming both from space-based X-ray and γ -ray observatories and from ground-based Cerenkov arrays. The most sensitive of these observatories, the Chandra X-ray Observatory, has discovered almost 10^4 X-ray sources within a $2 \times 0.8 \text{ deg}^2$ region near the Galactic center (Muno et al., 2009). The Chandra Galactic Bulge Survey (Bassa et al., 2008) contains about 10^3 X-ray sources spread over a larger, slightly less crowded region, and already has deep optical follow-up. These objects are often extinguished enough that they cannot be observed in the optical, but there are also often multiple infrared counterparts found even in moderately deep infrared images within the $1''$ or smaller Chandra error regions (e.g., Gosling et al., 2007). For γ -ray sources, such as those which have been found with INTEGRAL (e.g., Kuulkers et al., 2006; Bird et al., 2007) and HESS (Aharonian et al., 2007; Chaves et al., 2008), the point source localization is even poorer – typically several arcminutes. Fortunately, X-ray binaries are usually variable, and their variability in infrared and X-rays is, for the most part, well correlated (e.g., Russell et al., 2006). As a result an infrared variability survey of the inner Galaxy can be combined with the ongoing monitoring in X-rays and γ -rays from missions like Swift and MAXI, should give the opportunity to search narrow down the list of candidate infrared counterparts

through searches for IR emitters with variability well correlated with that in the high energy bands.

5. *To search for microlensing event*, especially reddened events, short time-scale events, and high magnification events in obscured high-density fields. The spatial dependence of the microlensing optical depth τ at near-infrared wavelengths has been modelled by Kerins et al. (2009) using synthetic population synthesis models of the Galactic disk and bulge. The spatial variation of τ can probe directly the mass distribution contained in the inner regions. Unfortunately, current optical microlensing searches do not cover the whole bulge or the plane due to the prevalence of dust. In particular, they miss the inner regions of the bulge where the optical depth is higher, providing poor constraints to current models (Bissantz & Gerhard, 2002; Bissantz et al., 2004). At near-IR wavelengths a map of microlensing optical depth for the whole bulge can be made, allowing a search for asymmetries in the spatial distribution of τ . The strength of the microlensing asymmetry is a function of the orientation of the inner bar as well as the relative contributions of the bulge and disk to the microlensing rate. A near-IR microlensing sample can therefore provide an important additional lever on the 3D geometry of the inner Galaxy. In addition, we expect to detect microlensing of stars in the Sgr dSph galaxy (e.g., Popowski et al., 2005).

6. *To monitor variability around the Galactic center*: an area of 1.5 deg^2 around the Galactic center including the 180 pc Nuclear Ring (Messineo et al., 2002) will be the most frequently monitored field, over a total of 200 epochs spanning five years. Expected variability due to high-magnification microlensing, or flares due to black-hole accretion, can occur (e.g., Chanamé et al., 2001). Black-hole flares easily reach $K_s \sim 16$ mag, with a typical duration of 10–30 min. The expected flare rate is 2–6 per day (Genzel et al., 2003; Eisenhauer et al., 2005), in addition to a longer-timescale variation predicted by accretion simulations (Cuadra et al., 2006). We also expect some Wolf-Rayet variability in the population of massive stars and clusters in this region, and we will search for eclipsing WR stars. In addition, we will be able to identify the counterparts of high-energy (γ -, and X-ray) sources: accreting black holes, microquasars, binary-pulsar companions, low mass X-ray binaries (LMXBs), and high mass X-ray binaries (HMXBs) (e.g., Mirabel & Rodríguez, 1998; Lucas et al., 2008). In particular, this survey may reveal the as yet undetected counterparts of the most luminous, persistent hard X-ray/jet sources in the Galactic center region, 1E 1740.7-2942 (Mirabel et al., 1992) and GRS 1758-258 (Rodríguez et al., 1992). Our survey will allow us to identify and monitor the counterparts of several variable high-energy sources, and perhaps in some cases to determine their orbital periods.

7. *To search for new star clusters of different ages and identify their variable star members*, such as Cepheids, semiregular variables, W UMa-, and δ Sct-type stars. The asymmetric distribution of the known globulars in the Galactic center region hints at the presence of additional, as yet undiscovered objects (Ivanov et al., 2005; Kurtev et al., 2008). Our team members have already carried out successful campaigns searching for new clusters in the 2MASS Point Source Catalogue (Ivanov et al., 2002; Borissova et al., 2003; Dutra et al., 2003). Note that 2MASS, with a $K_{s,\text{lim}} = 14.5$ mag in the bulge, discovered hundreds of open-cluster candidates, as well as two new globular clusters. Because we will reach 3 – 4 mag deeper, we expect to find many new clusters.

We will build a homogeneous sample of at least 300 open clusters in the direction of the Galactic center, with accurately derived fundamental parameters. A sample thus obtained will be useful to investigate the structure of the Galactic disk in directions intercepting the bulge. This will represent a major improvement over our current knowledge in this area, since only 20 clusters have so far been studied in detail in this region of the sky, according to the last update (ver. 2.10, 2009) of Dias’ catalogue of Galactic Open Clusters (Dias et al., 2002). We will carry out a census of the Milky Way open clusters projected onto the central parts of the Galaxy. This will allow us to establish the fraction of star clusters compared to statistical fluctuations of the dense stellar field in those directions, as well as the cluster-formation efficiency relative to field stars. We can also estimate the role of disruption effects on timescales < 10 Myr (particularly useful for open clusters). We will derive the physical parameters: angular sizes, radial velocities, reddening, distances, masses, and ages of these clusters. Reliable fundamental parameters of unstudied open clusters are important both to disk studies and to constrain the theories of molecular-cloud fragmentation, star formation, as well as stellar and dynamical evolution. We will trace the structure of the Galactic disk. Recent studies of the disk structure based on open clusters are complete up to only 1 kpc from the Sun. We will complement and re-derive the existing kinematics distributions such as distance of the cluster to the Galactic center *vs.* age distribution, open clusters age histogram, distance of the open clusters to the Sun *vs.* reddening, etc.

8. *To provide complementary near-IR multi-colour information* (reddening, temperatures, luminosities) and time coverage to the following past and on-going surveys: GLIMPSE-II, VPHAS+, MACHO, OGLE, EROS, MOA, Pan-STARRS1, and PLANET. Near-IR photometry is important for the events discovered by microlensing surveys. For old previously detected events or new ones, the VVV survey will give field reddening, a baseline colour, and a magnitude that can immediately be translated into temperature and luminosity for the source star. Char-

acterization of the source is essential for refining the microlensing light-curve parameters and the physical lens properties (e.g., Beaulieu et al., 2006).

9. *To find variable stars in the Sgr dSph galaxy:* Figure 7 shows that the Sgr dSph RR Lyrae are well within reach and can be readily identified. RR Lyrae would give the 3-D structure of the Sgr dSph (e.g., Alard, 1996; Alcock et al., 1998). To measure the depth and the tilt of the Sgr dSph along the line of sight, mean RR Lyrae magnitudes with an accuracy better than 0.01 mag are necessary. This corresponds to the tidal radius of M54, supposedly the core of the Sgr dSph galaxy (Monaco et al., 2004). We will also detect and measure carbon stars, semiregulars, and eclipsing binary members of the Sgr dwarf galaxy (type II Cepheids are expected in the bulge, but classical Cepheids are not; since these would be found in the disk instead).

10. *To identify high-proper motion objects and background Quasi-Stellar Objects (QSOs):* this goal links the – seemingly unrelated – intrinsically faintest and brightest objects in the Universe. On the faint end, we would use proper motions to find nearby late M-type stars, brown dwarfs (L and T types), and high-velocity halo stars. The proper motions of the most interesting low-mass objects will be determined using UKIDSS, DENIS, and 2MASS to extend the time baseline, and to search for objects with smaller proper motions. With an astrometric accuracy of ~ 10 mas, comparable to UKIDSS (e.g., Lodiou et al., 2007; Deacon et al., 2009), or slightly lower in the most crowded regions, we will be able to determine this proper motions (Lucas et al., 2008). Scaling the results of the UKIDSS proper motion studies we expect an accuracy of $\lesssim 15$ miliarcsec yr^{-1} . This is beyond the minimum value to distinguish bulge and disk populations, since the proper motion difference between them is ~ 6 miliarcsec yr^{-1} in the galactic center region (Clarkson et al., 2008).

On the intrinsically bright end, variability would also allow us to identify background quasars, providing an extragalactic reference scale for future proper motions (e.g., Piatek et al., 2005). QSOs have a relatively broad colour range depending on their redshift, and their intrinsic variability increases monotonically with increasing time lags (de Vries et al., 2005). Their amplitudes should be > 0.2 mag in the near-IR (Enya et al., 2002). We estimate that we will find > 500 active galactic nuclei (AGNs), assuming a surface density of 2 deg^{-2} with $K_s < 15.5$ mag (Leipski et al., 2005) in the regions above and below the disk where $A_K < 0.5$ mag.

11. *To identify pre-main-sequence (pre-MS) clusters and associations through variability:* neither the duration of pre-MS evolution as a function of mass nor the duration of active star formation in molecular clouds are well established. IR

studies (e.g. Carpenter et al., 2001) have shown that a large fraction of all pre-MS stars are variable over a wide range in absolute magnitude, therefore, the identification of young stellar objects (YSOs) via a variable survey is a suitable method to detect YSOs due to its independence on color. VVV will be capable of picking out loose associations of pre-MS stars in crowded fields long after the molecular cloud has dispersed and the cluster has become unbound. Through careful analysis of the detection rate of such dispersed pre-MS populations and comparison with the detection rate of pre-MS accretion disks with Spitzer and WISE it will be possible to determine the relative durations of the phases with and without a disk. Two such rare pre-MS variables, KH 15D and V1648 Ori, have been described by Herbst et al. (2002); Kusakabe et al. (2005) and Reipurth & Aspin (2004).

5 Conclusions

We have described our near-IR public survey of the inner Milky Way bulge and disk. The VVV is a survey to be carried out with VISTA at Paranal Observatory between 2010 and 2014. It will map repeatedly most of the Milky Way bulge, as well as the inner southern disk, covering a total area of about 520 deg² containing about $\sim 10^9$ point sources, 33 known globular clusters and more than three hundred known open clusters. The main survey products will be a $ZYJHK_s$ atlas of the Milky Way bulge and inner disk, and catalogues of variable point sources and high-proper-motion objects. The multi-epoch K_s -band photometry will allow the identification and phasing of periodic variable stars, as well as microlensing events and planetary transits. We will unveil the 3-D structure of the inner bulge and disk of the Milky Way using well understood distance indicators such as RR Lyrae stars, Cepheids, and red-clump giants. The survey is expected to detect more than 100 star forming regions and pre-MS clusters, benefiting from sensibility to variable pre-MS stars in regions where the molecular cloud has been dispersed. This large sample will permit measurement of the duration of the pre-MS evolution as a function of mass. It will also allow investigation of the effect of environment on the outcome of the star formation process. The VISTA observations will be combined with data from MACHO, OGLE, EROS, 2MASS, DENIS, HST, Spitzer, Chandra, INTEGRAL, AKARI, WISE, Fermi LAT, XMM-Newton and in the future GAIA and ALMA for a complete understanding of the variable star sources in the inner Milky Way.

Acknowledgements

We would like to thank Sebastián Ramírez-Alegría for providing us with NTT/SOFI data showed in the bottom panel of Fig. 5. This work is supported by MIDEPLAN's Programa Iniciativa Científica Milenio through grant P07-021-F, awarded to The Milky Way Millennium Nucleus; by the BASAL Center for Astrophysics and Associated Technologies PFB-06; by the FONDAP Center for Astrophysics N. 15010003; and by FONDECYT N. 1090213 and 1071002. R. H. Barbá, G. Gunthardt and M. Soto acknowledge support from CONICYT through Gemini Project N. 32080001. J. Borissova and R. Kurtev acknowledge support from FONDECYT N. 1080086 and 1080154. G. Pignata acknowledges support from the Millenium Center for Supernova Science through MIDEPLAN grant P06-045-F and Comit-Mixto ESO-Gobierno de Chile.

References

- Abadi, M. G., Navarro, J. F., Steinmetz, M., & Eke, V. R. 2003, *ApJ*, 591, 499
- Aharonian, F. A., Akhperjanian, A. G., Bazer-Bachi, A. R., et al. 2007, *A&A*, 469, L1
- Alcock, C., Allsman, R. A., Alves, D. R., et al. 1998, *ApJ*, 492, 190
- Alard, C. 1996, *ApJ*, 458, L17
- Alard, C., & Lupton, R. H. 1998, *ApJ*, 503, 325
- Alard, C. 2000, *A&AS*, 144, 363
- Altmann, M., Catelan, M., & Zoccali, M. 2005, *A&A*, 439, L5
- Bassa, C., et al. 2008, *The Astronomer's Telegram*, 1575, 1
- Beaulieu, J.-P., Bennett, D. P., Fouqué, P., et al. 2006, *Nature*, 439, 437
- Benjamin, R. A., et al. 2005, *ApJ*, 630, L149
- Bica, E., Dutra, C. M., Soares, J., & Barbuy, B. 2003, *A&A*, 404, 223
- Bird, A. J., et al. 2007, *ApJS*, 170, 175
- Bissantz, N., & Gerhard, O. 2002, *MNRAS*, 330, 591
- Bissantz, N., Debattista, V. P., & Gerhard, O. 2004, *ApJ*, 601, L155

- Bono, G., Caputo, F., & Di Criscienzo, M. 2007, *A&A*, 476, 779
- Bono, G., Castellani, V., & Marconi, M. 2000, *ApJL*, 532, L129
- Borissova, J., Pessev, P., Ivanov, V. D., et al. 2003, *A&A*, 411, 83
- Cacciari, C., Corwin, T. M., & Carney, B. W. 2005, *AJ*, 129, 267
- Carney, B. W., Fulbright, J. P., Terndrup, D. M., et al 1995, *AJ*, 110, 1674
- Carpenter, J. M., Hillenbrand, L. A., & Skrutskie, M. F. 2001, *AJ*, 121, 3160
- Catelan, M. 2004, *IAU Colloq. 193: Variable Stars in the Local Group*, eds. D.W.Kurtz & K.R.Pollard, (San Francisco ASP), 310, 11
- Catelan, M. 2004, *ApJ*, 600, 409
- Catelan, M., Smith, H. A., Pritzl, B. J., et al. 2006, *Mem. Soc. Astron. Italiana*, 77, 202
- Catelan, M. 2009, *Ap&SS*, 18
- Chanamé, J., Gould, A., & Miralda-Escudé, J. 2001, *ApJ*, 563, 793
- Chaves, R. C. G., Renaud, M., Lemoine-Goumard, M., & Goret, P. 2008, *American Institute of Physics Conference Series*, 1085, 372
- Clarkson, W., et al. 2008, *ApJ*, 684, 1110
- Collinge, M. J., Sumi, T., & Fabrycky, D. 2006, *ApJ*, 651, 197
- Cross, N. J. G., Collins, R. S., Hambly, N. C., Blake, R. P., Read, M. A., Sutorius, E. T. W., Mann, R. G., & Williams, P. M. 2009, *MNRAS*, 399, 1730
- Cuadra, J., Nayakshin, S., Springel, V., & di Matteo, T. 2006, *MNRAS*, 366, 358
- Deacon, N. R., Hambly, N. C., King, R. R., & McCaughrean, M. J. 2009, *MNRAS*, 394, 857
- Del Principe, M., Piersimoni, A. M., Bono, G., Di Paola, A., Dolci, M., & Marconi, M. 2005, *AJ*, 129, 2714
- de Vries, W. H., Becker, R. H., White, R. L., & Loomis, C. 2005, *AJ*, 129, 615
- Dias, W. S., Alessi, B. S., Moitinho, A., & Lépine, J. R. D. 2002, *A&A*, 389, 871
- Dias, W. S., Assafin, M., Flório, V., et al. 2006, *A&A*, 446, 949

Di Criscienzo, M., Caputo, F., Marconi, M., & Cassisi, S. 2007, *A&A*, 471, 893

Dutra, C. M., Bica, E., Soares, J., & Barbuy, B. 2003, *A&A*, 400, 533

Dutra, C. M., Ortolani, S., Bica, E., et al. 2003, *A&A*, 408, 127

Dwek, E., Arendt, R. G., Hauser, M. G., et al. 1995, *ApJ*, 445, 716

Eisenhauer, F., Genzel, R., Alexander, T., et al. 2005, *ApJ*, 628, 246

Emerson, J. P., Irwin, M. J., Lewis, J., et al. 2004, *Proc. SPIE*, 5493, 401

Enya, K., Yoshii, Y., Kobayashi, Y., et al. 2002, *ApJS*, 141, 45

Fiorentino, G., Limongi, M., Caputo, F., & Marconi, M. 2006, *A&A*, 460, 155

Fiorentino, G., Marconi, M., Musella, I., & Caputo, F. 2007, *A&A*, 476, 863

Feast, M. W., Laney, C. D., Kinman, T. D., van Leeuwen, F., & Whitelock, P. A. 2008, *MNRAS*, 386, 2115

Fouque, P., & Gieren, W. P. 1997, *A&A*, 320, 799

Genzel, R., Schödel, R., Ott, T., et al. 2003, *Nature*, 425, 934

Gieren, W., Storm, J., Barnes, T. G., III, Fouqué, P., Pietrzyński, G., & Kienzle, F. 2005, *ApJ*, 627, 224

Gosling, A. J., Bandyopadhyay, R. M., Miller-Jones, J. C. A., & Farrell, S. A. 2007, *MNRAS*, 380, 1511

Gosling, A. J., Bandyopadhyay, R. M., & Blundell, K. M. 2009, *MNRAS*, 394, 2247

Hambly, N. C., Mann, R. G., Bond, I., et al. 2004, *Proc. SPIE*, 5493, 423

Harris, W. E. 1996, *AJ*, 112, 1487

Herbst, W., et al. 2002, *PASP*, 114, 1167

Hodgkin, S. T., Irwin, M. J., Hewett, P. C., & Warren, S. J. 2009, *MNRAS*, 394, 675

Ibata, R. A., Gilmore, G., & Irwin, M. J. 1995, *MNRAS*, 277, 781

Irwin, M. J., Lewis, J., Hodgkin, S., 2004, *Proc. SPIE*, 5493, 411

- Ivanov, V. D., Borissova, J., Pessev, P., et al. 2002, *A&A*, 394, L1
- Ivanov, V. D., Kurtev, R., & Borissova, J. 2005, *A&A*, 442, 195
- Jones, R. V., Carney, B. W., & Fulbright, J. P. 1996, *PASP*, 108, 877
- Kaluzny, J., Olech, A., Thompson, I. B., et al. 2004, *A&A*, 424, 1101
- Kerins, E., Robin, A. C., & Marshall, D. J. 2009, *MNRAS*, 396, 1202
- Kerschbaum, F., Groenewegen, M. A. T., & Lazaro, C. 2006, *A&A*, 460, 539
- Kormendy, J., & Kennicutt, R. C., Jr. 2004, *ARA&A*, 42, 603
- Kuijken, K., & Rich, R. M. 2002, *AJ*, 124, 2054
- Kurtev, R., Ivanov, V. D., Borissova, J., & Ortolani, S. 2008, *A&A*, 489, 583
- Kusakabe, N., et al. 2005, *ApJ*, 632, L139
- Kuulkers, E., Shaw, S. E., Brandt, S., et al. 2006, *The Transient Milky Way: A Perspective for MIRAX*, 840, 30
- Leipski, C., Haas, M., Meusinger, H., et al. 2005, *A&A*, 440, L5
- Lodieu, N., et al. 2007, *MNRAS*, 379, 1423
- Lonsdale, C. J., et al. 2009, *arXiv:0903.1828*
- López-Corredoira, M., Cabrera-Lavers, A., & Gerhard, O. E. 2005, *A&A*, 439, 107
- López-Corredoira, M., Cabrera-Lavers, A., Mahoney, T. J., Hammersley, P. L., Garzón, F., & González-Fernández, C. 2007, *AJ*, 133, 154
- Lucas, P. W., et al. 2008, *MNRAS*, 391, 136
- Majewski, S. R., et al. 2007, *Bulletin of the American Astronomical Society*, 38, 962
- Marconi, M., Caputo, F., Di Criscienzo, M., & Castellani, M. 2003, *ApJ*, 596, 299
- Marconi, M., & Degl'Innocenti, S. 2007, *A&A*, 474, 557
- Matsunaga, N., Kawadu, T., Nishiyama, S., Nagayama, T., Hatano, H., Tamura, M., Glass, I. S., & Nagata, T. 2009, *MNRAS*, 399, 1709

- McPherson, A. M., Born, A., Sutherland, W., et al. 2006, *Proc. SPIE*, 6267, 7
- Meléndez, J., et al. 2008, *A&A*, 484, L21
- Merrifield, M. R. 2004, *Milky Way Surveys: The Structure and Evolution of our Galaxy*, 317, 289
- Messineo, M., Habing, H. J., Sjouwerman, et al. 2002, *A&A*, 393, 115
- Minniti, D., Alcock, C., Allsman, R. A., et al. 1999, *The Third Stromlo Symposium: The Galactic Halo*, 165, 284
- Mirabel, I. F., Rodríguez, L. F., Cordier, B., et al. 1992, *Nature*, 358, 215
- Mirabel, I. F., & Rodríguez, L. F. 1998, *Nature*, 392, 673
- Monaco, L., Bellazzini, M., Ferraro, F. R., & Pancino, E. 2004, *MNRAS*, 353, 874
- Muno, M. P., et al. 2009, *ApJS*, 181, 110
- Nishiyama, S., Nagata, T., Baba, D., et al. 2005, *ApJ*, 621, L105
- Nishiyama, S., et al. 2006, *ApJ*, 638, 839
- Piatek, S., Pryor, C., Bristow, P., et al. 2005, *AJ*, 130, 95
- Pietrukowicz, P., Kaluzny, J., Thompson, et al. 2005, *Acta Astron.*, 55, 261
- Pietrukowicz, P., et al. 2009, *A&A*, 503, 651
- Popowski, P., Griest, K., Thomas, C. L., et al. 2005, *ApJ*, 631, 879
- Pritzl, B. J., Smith, H. A., Catelan, M., & Sweigart, A. V. 2000, *ApJ*, 530, L41
- Pritzl, B. J., Smith, H. A., Stetson, P. B., et al. 2003, *AJ*, 126, 1381
- Ree, C. H., Yoon, S.-J., Rey, S.-C., & Lee, Y.-W. 2002, *Omega Centauri, A Unique Window into Astrophysics*, 265, 101
- Reipurth, B., & Aspin, C. 2004, *ApJ*, 606, L119
- Rieke, G. H., & Lebofsky, M. J. 1985, *ApJ*, 288, 618
- Rodríguez, L. F., Mirabel, I. F., & Martí, J. 1992, *ApJ*, 401, L15
- Russell, D. M., Fender, R. P., Hynes, R. I., Brocksopp, C., Homan, J., Jonker, P. G., & Buxton, M. M. 2006, *MNRAS*, 371, 1334

Schuller, F., Omont, A., Glass, I. S., Schultheis, M., Egan, M. P., & Price, S. D. 2006, *A&A*, 453, 535

Silva Aguirre, V., Catelan, M., Weiss, A., & Valcarce, A. A. R. 2008, *A&A*, 489, 1201

Skrutskie, M. F., et al. 2006, *AJ*, 131, 1163

Smith, B. J., Price, S. D., & Moffett, A. J. 2006, *AJ*, 131, 612

Stanek, K. Z., Mateo, M., Udalski, A., et al. 1994, *ApJ*, 429, L73

Torres, G., & Ribas, I. 2002, *ApJ*, 567, 1140

Udalski, A., Szewczyk, O., Żebruń, K., et al. 2002, *Acta Astron.*, 52, 317

Weldrake, D. T. F., & Bayliss, D. D. R. 2008, *AJ*, 135, 649

Woźniak, P. R., Udalski, A., Szymański, M., et al. 2002, *Acta Astron.*, 52, 129

Yusef-Zadeh, F., et al. 2009, *ApJ*, 702, 178

Zoccali, M., Renzini, A., Ortolani, S., et al. 2003, *A&A*, 399, 931

Zoccali, M., Lecureur, A., Barbuy, B., et al. 2006, *A&A*, 457, L1

¹ Departamento de Astronomía y Astrofísica, Pontificia Universidad Católica de Chile, Av. Vicuña Mackenna 4860, Casilla 306, Santiago 22, Chile

² Vatican Observatory, Vatican City State V-00120, Italy

³ Centre for Astrophysics Research, Science and Technology Research Institute, University of Hertfordshire, Hatfield AL10 9AB, UK

⁴ Astronomy Unit, School of Mathematical Sciences, Queen Mary, University of London, Mile End Road, London, E1 4NS, UK

⁵ Nicolaus Copernicus Astronomical Center, ul. Bartycka 18, 00-716 Warszawa, Poland

⁶ Observatorio Astronómico de Córdoba, Universidad Nacional de Córdoba, Laprida 854, 5000 Córdoba, Argentina

⁷ European Southern Observatory, Av. Alonso de Córdoba 3107, Casilla 19, Santiago 19001, Chile

⁸ Consejo Nacional de Investigaciones Científicas y Técnicas, Av. Rivadavia 1917 - CP C1033AAJ - Buenos Aires, Argentina

⁹ Department of Astronomy, University of Michigan, Ann Arbor, MI 48109-1090, USA

¹⁰ Departamento de Física, Universidad de La Serena, Benavente 980, La Serena, Chile

¹¹ Department of Astronomy, University of Florida, 211 Bryant Space Science Center P.O. Box 112055, Gainesville, FL, 32611-2055, USA

- ¹² Universidade de São Paulo, IAG, Rua do Matão 1226, Cidade Universitária, São Paulo 05508-900, Brazil
- ¹³ Space Telescope Science Institute, 3700 San Martin Drive, Baltimore, MD 21218, USA
- ¹⁴ Universidade Federal do Rio Grande do Sul, IF, CP 15051, Porto Alegre 91501-970, RS, Brazil
- ¹⁵ Departamento de Física y Astronomía, Facultad de Ciencias, Universidad de Valparaíso, Ave. Gran Bretaña 1111, Playa Ancha, Casilla 5030, Valparaíso, Chile
- ¹⁶ Departamento de Astronomía, Universidad de Chile, Casilla 36-D, Santiago, Chile
- ¹⁷ Institute for Astronomy, The University of Edinburgh, Royal Observatory, Blackford Hill, Edinburgh EH9 3HJ, UK
- ¹⁸ The Department of Physics and Astronomy, University of Sheffield, Hick Building, Hounsfield Road, Sheffield, S3 7RH, UK
- ¹⁹ National Astronomical Observatories, Chinese Academy of Sciences, 20A Datun Road, Chaoyang District, Beijing 100021, China
- ²⁰ Konkoly Observatory of the Hungarian Academy of Sciences, H-1525 Budapest, PO Box 67, Hungary
- ²¹ Astrophysics Group, Imperial College London, Blackett Laboratory, Prince Consort Road, London SW7 2AZ, UK
- ²² Facultad de Ciencias Astronómicas y Geofísicas, Universidad Nacional de La Plata, and Instituto de Astrofísica La Plata, Paseo del Bosque S/N, B1900FWA, La Plata, Argentina
- ²³ Departamento de Astronomía, Universidad de Concepción, Casilla 160-C, Concepción, Chile
- ²⁴ Max Planck Institute for Astronomy, Königstuhl 17, 69117 Heidelberg, Germany
- ²⁵ European Southern Observatory, Karl-Schwarzschild-Strasse 2, D-85748 Garching, Germany
- ²⁶ Institute of Astronomy, University of Cambridge, Madingley Road, Cambridge CB3 0HA, UK
- ²⁷ Jodrell Bank Centre for Astrophysics, The University of Manchester, Oxford Road, Manchester M13 9PL, UK
- ²⁸ Instituto de Astrofísica de Canarias, Vía Láctea s/n, E38205 - La Laguna (Tenerife), Spain
- ²⁹ School of Physics and Astronomy, University of Southampton, Highfield, Southampton, SO17 1BJ, UK
- ³⁰ Istituto di Astrofisica Spaziale e Fisica Cosmica di Bologna, via Gobetti 101, 40129 Bologna, Italy
- ³¹ Chester F. Carlson Centre for Imaging Science, Rochester Institute of Technology, 54 Lomb Memorial Drive, Rochester NY 14623, USA
- ³² The Astrophysics and Fundamental Physics Missions Division, Research and Scientific Support Department, Directorate of Science and Robotic Exploration, ESTEC, Postbus 299, 2200 AG Noordwijk, the Netherlands
- ³³ Service d'Astrophysique - IRFU, CEA-Saclay, 91191 Gif sur Yvette, France
- ³⁴ Instituto de Astronomía y Física del Espacio, Casilla de Correo 67, Sucursal 28, Buenos Aires, Argentina
- ³⁵ Dipartimento di Astronomia, Università di Padova, vicolo dell'Osservatorio 3, 35122 Padova, Italy

³⁶ Departamento de Ciencias Físicas, Universidad Andrés Bello, Av. República 252, Santiago, Chile

³⁷ Department of Physics & Astronomy, University of Leicester, University Road, Leicester, LE1 7RH, UK

³⁸ Hartebeesthoek Radio Astronomy Observatory, PO Box 443, Krugersdorp 1740, South Africa

³⁹ The University of Kent, Canterbury, Kent, CT2 7NZ, UK

⁴⁰ Division of Optical and Infrared Astronomy, National Astronomical Observatory of Japan 2-21-1 Osawa, Mitaka, Tokyo, 181-8588, Japan